



Electrical properties and applications of carbon based nanocomposite materials: An overview

R. Sanjinés^{a,*}, M.D. Abad^b, Cr. Vâju^a, R. Smajda^a, M. Mionić^a, A. Magrez^a

^a Institute of Condensed Matter Physics, EPFL, CH-1015 Lausanne, Switzerland

^b Instituto de Ciencia de Materiales de Sevilla, CSIC-US, Sevilla 4109, Spain

ARTICLE INFO

Available online 16 January 2011

Keywords:

Carbon based nanocomposites
Thin films
Electrical properties
Carbon nanotubes
Graphene
Carbon black

ABSTRACT

The allotropic forms of carbon (amorphous and polycrystalline graphite, carbon black, fullerenes, nanotubes, graphene) exhibit a large variety of charge transport properties which have been stimulating fundamental and applied research for the development of new devices based on micro and nano-sized electronic systems. Carbon based nanocomposites offer the possibility to improve the device performances and to develop novel multifunctional material systems by combining the properties of each individual phase. In this paper we review the electrical properties of carbon materials and some of the most exciting carbon based nanocomposites, as well as their potential technological applications. First, the electrical properties of amorphous and polycrystalline graphitic materials and those of their related nanocomposites materials are discussed. Second, an overview of the state-of-art on research and applications of carbon nanotube-based composites is presented. Third, we discuss briefly the emerging area of research related to graphene materials. Finally, the electrical properties and applications of conducting carbon black aggregates and carbon black/polymer composites are overviewed.

© 2011 Elsevier B.V. All rights reserved.

1. Introduction

The electrical properties of carbon based nanostructured composite materials are intimately related to the electronic properties of their constituting components. Nanocomposites are complex materials. In addition to the intrinsic properties of each individual phase (including particle sizes, defect density...), grain boundaries as well as interfaces play a pivotal role in the overall physical and chemical properties of composites. From a technological point of view, the combination of two materials is particularly useful to integrate the properties of the two components in a hybrid material. Thus, they can be used in catalysis, nanoelectronics, energy storage, gas sensors, solar cells, to name but a few. The review presented in this paper includes the most relevant published data in order to give a general synopsis on the electrical properties of different carbon phases and on the applications of carbon based composite materials to be developed. Obviously, due to the vast number of papers published in the literature the present overview cannot be exhaustive but it highlights the intrinsic coupling of electrical properties and development of devices in carbon based nanocomposite materials.

2. Carbon polymorphic forms

Beside the well-known diamond and graphite crystalline phases, carbon exhibits many forms such as fullerene molecules, nanotubes, graphene, semi-crystalline phase such as carbon black, and diverse amorphous phases [1–4]. In cubic diamond phase, each carbon atom is bonded to four other carbons by strong sp^3 covalent bonds. With no conduction electrons, diamond has very low electrical conductivity. Graphite is formed by stacking flat sheets of sp^2 -bonded carbon atoms in a two-dimensional (2D) hexagonal lattice, the sheets are weakly bonded between each other by van der Waals forces. Graphite is a semi-metal due to the narrow band overlap (about 40 meV) of valence and conduction bands. Fullerene C_{60} was the most investigated man made C phase before the discovery of carbon nanotubes and more recently graphene. A molecule of C_{60} is a truncated icosahedron structure having 20 hexagons and 12 pentagons with a perfect symmetry in the sense that every C atom is a vertex of one pentagon and two hexagons. Pure C_{60} is semiconducting (1.8 eV band gap), however superconductivity can be induced by charge doping [1,2].

Carbon nanotubes (CNTs) are often described as rolled-up graphene sheet into a cylinder along a direction defined by the chiral vector $\mathbf{c} = n\mathbf{a}_1 + m\mathbf{a}_2$ where \mathbf{a}_1 and \mathbf{a}_2 are the unit vectors of the graphene hexagonal lattice (n and m are integers). Single-walled carbon nanotubes (SWCNT) and Multi-walled carbon nanotubes (MWCNT) are built from one or few, respectively single layer of graphene. In a MWCNT, the interlayer distance is about 0.34 nm.

* Corresponding author. Tel.: +41 216934442; fax: +41 216934666.
E-mail address: rosendo.sanjines@epfl.ch (R. Sanjinés).

Depending on their structural symmetry, which is described by the terms armchair or zigzag configuration, carbon nanotubes can exhibit metallic or semiconducting behavior [2,3].

Graphene is a two dimensional single sheet of carbon atoms and is the thinnest existing materials. Because of its 2D character graphene exhibits peculiar electrical properties; electrons behave as Dirac fermions and they, as well as holes exhibit high mobility (10,000 cm²/Vs at 300 K). According to the band structure calculations, the valence band (fully occupied) and the conduction band (empty band) touch at 6 points making graphene to be a zero-gap semiconductor [4].

3. Amorphous and nanocrystalline carbon films

3.1. Electrical properties

The electronic properties of carbon thin films are intimately depending on their physical structure. Hydrogenated or non-hydrogenated carbon films, often referred to as diamond-like carbon (DLC) films, can be either amorphous or nanocrystalline materials and contain both sp³ diamond and sp² graphite bonds. Amorphous carbon films containing predominantly sp² bonds are known as graphite-like amorphous carbon (GAC) films. The physical properties of DLC and GAC films are strongly influenced by the ratio of sp² sites to sp³. In particular the bonding and antibonding electronic states arising from the π bonds of carbon sp² sites determine the electrical properties of these materials [5–8]. They exhibit a wide range of DC electrical conductivity values at room temperature (from 10⁻¹⁴ to 10¹ S/m) and their temperature dependence can be dominated by thermally activated process with $\sigma = \sigma_0 \exp(-\Delta E/kT)$ and/or by hopping transport mechanisms. Among the theoretical models the variable range hopping (VRH) model is the most commonly used [9]. For instance, Zhao et al. [10] reported that in the graphitization process of the activated carbon treated by high-pressure sintering, the electrical properties are strongly correlated with structural features. The conductivity can change from 1-dimensional (1D) to 3-dimensional (3D) depending on the thermal treatment temperature. In samples treated below 1000 °C under high pressure conditions, VRH is observed as the main conduction mechanism. In 1D VRH, the relationship of resistivity ρ versus temperature T follows the relation $\rho = \rho_0 \exp\left(\frac{T_0}{T}\right)^x$ with $x = 1/2$, T_0 is related to the localization length ξ of the wave function. When nanoparticles are large enough, the 2D (with $x = 1/3$) or 3D ($x = 1/4$) VRH conduction mechanisms are observed indicating that 1D connections change to 2D or 3D. The insulator–metal transition appears between non-graphitized region and the almost-graphitized region. In the near graphitized region an approximately linear ρ – T relationship between resistivity and temperature is observed and the material exhibits semimetallic behavior. At higher sintering temperatures (1200–1600 °C) the graphitized activated carbon behaves as non-Fermi liquid and the resistivity exhibits a power law $\rho = A + BT^{3/2}$ [10].

The role of hydrogen on the concentration of localized states in hydrogenated DLC films has been discussed by Staryga et al. [8]. Since sp² configurations are associated to localized states, the effects of nitrogen doping on the electrical transport characteristics have also been investigated in amorphous CN_x films. The drastic changes in the electrical properties (about 3 orders of magnitude) observed in a-CN_x films as a function of the N concentration have been correlated to the bonding ability of N atoms to C sp² and to C sp³ sites and thus, leading to the modification of the density of the localized states [11]. The dynamics of hopping transport in a-CN_x was also investigated by AC electrical spectroscopic measurements [12–14].

3.2. DLC and GAC based nanocomposites

DLC and GAC films have been investigated because of their promising applications in electron field emission devices. In particular

they are good candidates for cold-cathode materials in field emission display technologies [15,16]. To avoid surface oxidation drawback, the incorporation of boron has been found to be an efficient way to improve the oxidation resistance of various carbon-based materials. In DLC films depending on the boron content, the nanocomposites are constituted of boron nanoparticles embedded in amorphous or nanocrystalline DLC matrix. The electrical conduction was described in terms of Mott VRH in localized states near the Fermi level [17,18].

The porosity and the relatively low reactivity of DLC and GAC make them ideal candidates as hosting matrix for neutral or electron donor nanoparticle species for preparing hybrid materials for catalytic applications. In catalysis, many studies have also been devoted to the synthesis of CNTs decorated with metal nanoparticles [19,20]. However DLC and GAC remain better candidates than CNT due to their low cost of production. Papadimitriou et al. [21] have recently investigated the catalytic properties of bimetallic samples Pt- and Au-coated Cu, Fe, Co, and Ni deposited on glassy carbon substrates by electrodeposition. In energy storage devices with high energy density like Li-ion batteries, V₂O₅/carbon composites have been considered to improve their high-rate performances. The high-rate discharge capacity properties have been investigated for various C materials and particle sizes [22].

3.3. Amorphous C in hard nanocomposite coatings

In the case of nanocomposite thin films based on amorphous C (a-C) and nanocrystalline hard materials (TiC_x, WC_x, TaC_x, TiBC_x...), which find many applications as new functional coatings, little is known about the role of C atoms on their electrical properties. It is expected that C segregation at the grain boundaries yields to the formation of inter-grains layer and can be the source of important modifications in the electrical properties of these films. The inter-grains layer could be either conducting or insulating and composed of single or binary compounds. DC resistivity measurements as a function of temperature can corroborate experimentally the structural evolution (grain size, thickness of the insulating or conducting layer) of the composite films. To illustrate these facts, in Fig. 1 we show the resistivity changes due to structural modifications in WC/a-C nanocomposites. The resistivity vs. temperature curves exhibit characteristics of low degree crystallized materials where scattering of electrons against grain boundaries and point defects become important. In such nanocomposites, the experimental results can be perfectly described by the grain boundary scattering model [23]. In this model, the electrical resistivity is given by

$$\rho_g = \left(\frac{m_e^* v_F}{Ne^2}\right) \left(\frac{1}{L}\right) G^{-(L/D)} = \left(\frac{K}{L}\right) G^{-(L/D)}$$

where m_e^* is the effective mass of the charger carriers, v_F is the Fermi velocity, N is the charge carrier density, D is the grain-size parameter, L is the inner-crystalline mean free path, and G is the mean probability for electrons to pass a single grain boundary. L contains the temperature-invariant elastic scattering free path, l_e , and the temperature-dependent inelastic scattering l_{in} , such that $L^{-1} = l_e^{-1} + l_{in}^{-1}$. Fig. 1B summarizes the principal parameters obtained for the fit. First, the grain sizes D deduced by the model agree well with crystallite sizes estimated from XRD and TEM experiments. Second, the calculated small l_e values are in agreement with the quasi-amorphous and nanocrystalline nature of these films indicating that the films contain high density of point defects. Third, the main parameter controlling the transport properties of these films seems to be the grain size, D changing from 2.3 to 6.0 nm. In quasi-amorphous materials, the grain boundaries vanish and the electron scattering is mainly dominated by the high density of point defects, this explains the large G values obtained from the fitting procedure. In contrast, both the grain boundary regions and point defects contribute to the electron

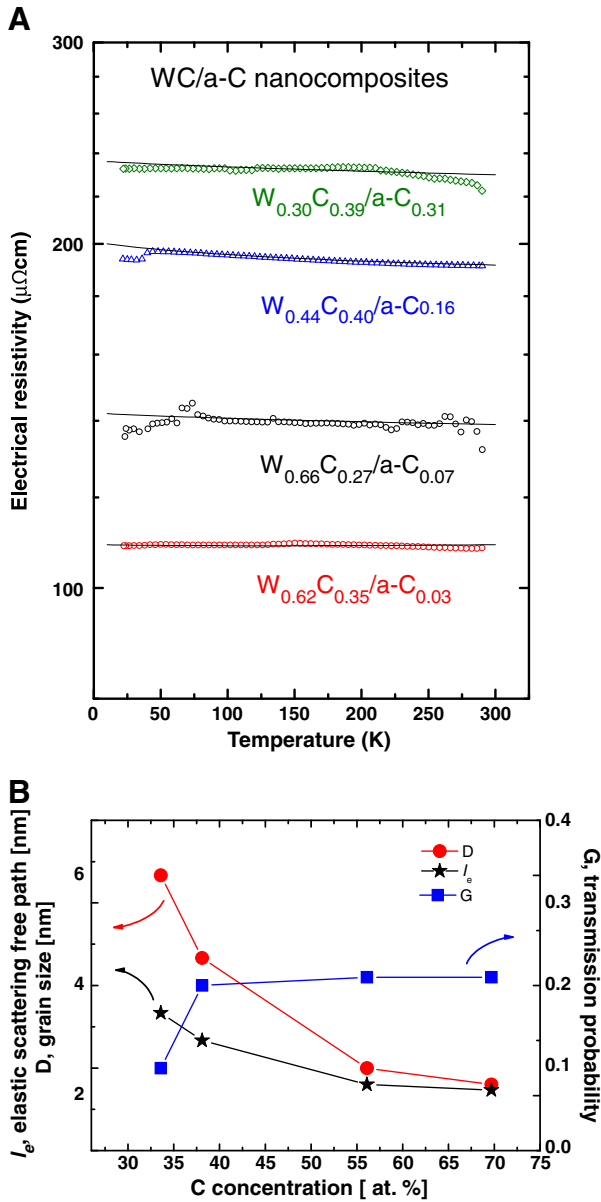


Fig. 1. A) Electrical resistivity vs. temperature of a-C/WC nanocomposites. The solid lines are the best fit with the grain-boundary model. B) Elastic scattering free path l_e , grain size D and transmission probability G deduced from the model as a function of the carbon atomic concentration.

scattering in nanocrystalline films with small crystallites sizes; the effect of the grain boundaries is noticeable by the diminution of the transmission probability. A detailed investigation for a-C/WC nanocomposite films has been reported elsewhere [24].

4. Carbon nanotubes

Due to their exceptional electronic and structural properties (metal or semiconductor, large surface areas, quantum effects connected with their nano-sized structure) CNTs have been considered as promising material for many electronic devices. Applications include thin film transistors and diodes, electrodes in optoelectronic devices, chemical and biosensors, electronic switching, etc [4,25–28]. In the frame of our research work, part of our activities is focused on the fabrication and characterization of CNTs. Much attention has been paid to the synthesis of carbon nanotubes as well as on organized and complex MWCNT structures. The most suitable method for the production of CNTs in mass and at low cost or directly on devices is

the catalytic chemical vapor deposition (CCVD) process. Since recent years, tremendous progresses have been made such as kilogram of CNTs can be produced per day at very low cost using standard laboratory equipments [29,30]. On the other hand, MWCNT vertically orientated to the surface substrate can also be grown. The density of MWCNT within the CNT “carpets” is around 10^{11} tubes cm^{-2} (see Fig. 2). In order to preserve the catalyst activity when millimeter thick CNT carpets are produced, traces amount of weak oxidizer is introduced into the reactor together with the carbon source. It is believed that the amorphous carbon is oxidized during the growth reducing the rate of catalyst poisoning [31].

The electrical properties of MWCNT carpets have been investigated by four-point measurements. As shown in Fig. 3, the electrical measurements were performed either perpendicular or parallel to the growth direction of the nanotubes. In both directions, the resistivity unambiguously exhibits the 2D Mott VHR behavior $\rho = \rho_0 \exp\left(\frac{T_0}{T}\right)^x$ with $x = 0.31–0.34$. No significant room temperature conductivity difference was observed between the two different orientations. However, a slightly faster increase of the resistivity with decreasing temperature in the perpendicular configuration was observed. The 2D Mott VHR behavior observed in our carpet films can be explained by the fact that conduction parallel to the MWCNT is a low resistivity

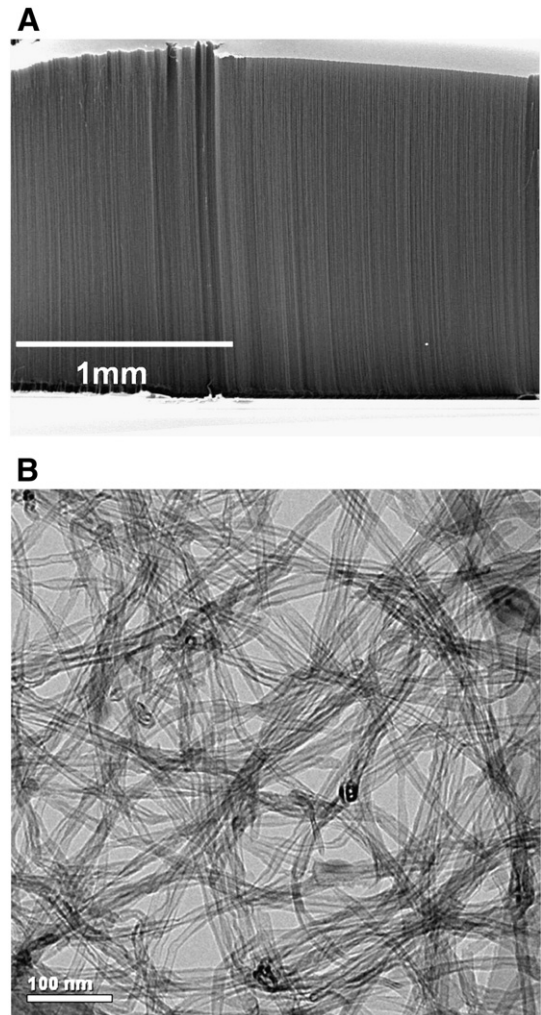


Fig. 2. A) Carbon nanotubes carpets produced over Fe (1 nm film) supported by Al_2O_3 (10 nm) deposited on Si wafer. The growth is performed at 750 °C and ethylene is used as carbon source. B) Scanning electron micrograph shows that millimetre long CNTs can be produced. CNTs are multiwalled with about 5 to 10 walls as can be seen in the transmission electron micrograph.

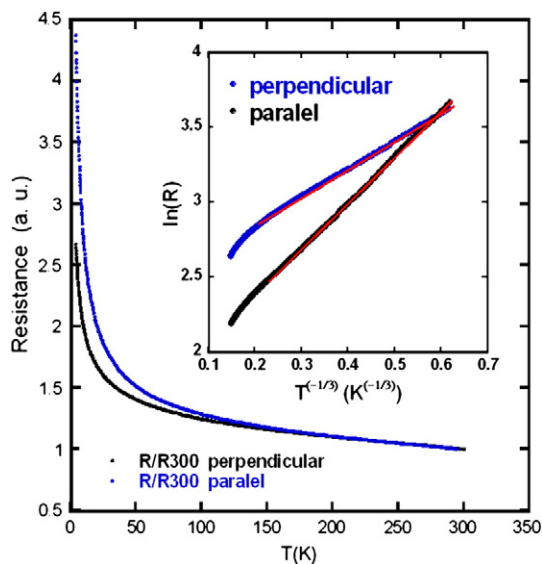


Fig. 3. Four points resistivity of CNT carpet in two configurations: parallel and perpendicular to the tube growth direction. Inset shows the behavior of $\ln(R)$ as function of $T^{-1/3}$, to illustrate the 2D Mott behavior. In the temperature range of 200 K to 6 K, the best fits using the relation $\rho = \rho_0 \exp\left(\frac{E_p}{T}\right)^\chi$ lead to $\chi = 0.311$ and $\chi = 0.336$ for parallel and perpendicular configurations.

metallic one but the global results are mainly dominated by the in-plane (xy) hopping between the MWCNT. These results show that if conductive CNT carpets are needed it could be necessary to improve the growing process or to add a second phase in order to increase their electrical conductivity (see below).

4.1. CNTs in conductive nanocomposites

CNTs can be used as a dispersed conductive phase in an insulating polymer matrix. The electrical conductivity of such composites is usually discussed in terms of percolation theory; the electrical volume conductivity is given by the percolation scaling law $\sigma(p) = \sigma_0(p - p_c)^t$ where p_c is the percolation threshold concentration and t the critical exponent [32–35]. Below the critical volume fraction the conductivity of the composite remains electrically insulating because the conductive particles are dispersed or grouped into small clusters. Above a critical volume fraction, the conductivity increases by many orders of magnitude. The values for the exponent t , observed for polymers filled with carbon black, carbon fibers, CNTs and graphene sheets, are typically in the range of 1 to 4. The percolation threshold coincides with the formation of a continuous network of conductive particles in the insulating matrix. For example, in polyamide 6.6-MWCNT composites a percolation threshold of 1.0 wt.% MWCNT was found [36]. In epoxy resin-based CNTs composites it was shown that the addition of less than 1.0 wt.% of CNTs into epoxy improves the electrical conductivity of the composite from around 10^{-11} to 10^{-1} S/m [37–39]. The conductivity is mainly restricted by the contact resistance of the CNT junctions [40,41]. It is also reported that the addition of about 0.1 wt.% of Ag can significantly improve the contact resistance of the CNT junctions in the polymer matrix increasing the conductivity by more than four orders of magnitude [42]. Finally, the number of studies reporting on the electrical properties of nanocomposites based on CNT carpets is rather limited. The effect of CNT alignment on percolation conductivity in CNT/polymer composites has been investigated by Du et al. [43]. Recently Silva et al. [44] have reported that CNTs alignment within polymer matrix resulting of the impregnation of carbon nanotube carpets yields to the enhancement of the conductivity (1.5×10^2 S/m) by two orders of magnitude as compared to the conductivity of composite with randomly oriented CNTs.

4.2. Organic solar cells

Transparent conducting electrodes based on CNTs have been investigated as alternative material to indium tin oxide (ITO) electrodes in organic solar cell and LEDs [45–51]. SWCNT and MWCNT exhibit intrinsic work functions values in the range of 3.4–4.0 eV and 4.5–5.1 eV, respectively, which are comparable to that of the ITO films (4.3 eV). Therefore, SWCNT and MWCNT can be used in bulk donor–acceptor type of solar cells, particularly by combining with π -conjugated polymers. In organic materials, the photon absorption causes a delocalization of the excited states generating excitons (electron-hole pairs). In such solar cells, CNTs act as electron acceptors, enhance the exciton dissociation by providing high field at the nanotube/polymer interface, and improve the transport of holes. Similar effect has been observed not only by dispersing double-walled carbon nanotubes in the polymer layer of P3HT or P3OT/n-Si heterojunction solar cells but also by incorporating oxidized MWCNT in the P3OT layer of region regular P3OT/n-Si heterojunction solar cell [50,51]. CNTs have many advantages compared to ITO films: low cost fabrication, resistant to attack of strong acids, porous electrodes on flexible and non-flexible electrodes.

4.3. CNTs in catalysis and energy storage devices

Since open ended or opened CNTs can be produced by chemical or physical processes. CNTs have been considered as ideal support for metal nanoparticles. Ag nanoparticles deposited on CNTs gained significant attention due to their potential applications as catalyst [52,53]. In energy storage devices, CNTs have been considered as potential anode material for Li-ion batteries [54–57]. However, pure CNTs electrodes exhibit high irreversibility capacity loss in the first cycle. The cycling stability can be improved using carbon-based composites, such Si-, Sn-, SnO-, SnSb_{0.5}-, and TiO₂-CNTs. Recently it was reported by Yan et al. [57] that the addition of Ag to TiO₂-CNTs electrodes leads to better cycling stability and higher reversible capacity (up to 272 mAh/g after 30 cycles), the increase of the electronic conductivity is accompanied by an efficient transfer of Li-ion in the composite structure.

4.4. Gas and biological sensors

CNT materials find as well a lot of application in chemical and biological sensor devices [28,58–69]. Pure SWCNT can exhibit drastic changes on electrical conductance when exposed to NH₃, NO₂ or O₂ gases. The sensing mechanisms have been attributed to the charge transfer of adsorbates [58,59]. However the charge sensitive conductance in SWCNTs is limited, like in graphite the sidewalls of pure CNTs are relatively non-reactive. Therefore, a novel strategy has been developed to alter the electronic properties of pure CNTs. Thus, a series of functionalization schemes have been proposed [67–69]. SWCNT decorated with transition metal (Pt, Pd, Rh) nanoparticles are able to detect hydrogen, methane and CO [65,66]. Recently, composites based on CNTs and polymers have been considered as interesting gas sensing materials [25,67–69]; SWCNT and MWCNT grafted with different polymers have been prepared and are able to detect vapors of several organic solvents such as dichloromethane, chloroform, acetone, as well as inorganic substances like HCl [69].

On the other hand, CNTs exhibit higher surface area than amorphous glassy carbon, they are therefore more suitable substrate for studying the immobilization or growth of biomolecules. Daniel et al. [27] have recently reviewed various aspects on the functionalization/grafting of DNA onto SWCNT and MWCNT with or without self-assembly which can be employed in fabricating biosensors for selective recognition of DNA. The advantage of the CNT based chemical sensors is that they can operate at room temperature with fast response time, they exhibit relatively high sensitivity, good selectivity and reversibility, and they are able to detect a large number of diver gases.

5. Graphene

Since the successful isolation of graphene layers by simple mechanical exfoliation, the fundamental properties of the single flat monolayer of graphite have been intensively investigated [4,70–83]. Graphene exhibits excellent electronic properties: high carrier mobility, ballistic transport, quantum Hall effect at room temperature, and good mechanical and chemical stability. Therefore, graphene has attracted interest for many applications. It is considered as promising material particularly for nanoelectronic and optoelectronic devices [4,70–73], in spintronics [74], in bio- and chemical sensors [75], quantum computing [76], etc. Many chemical routes to synthesize graphene at large scale have been developed including epitaxial growth on SiC [70,71], chemical vapor deposition [77–79], and graphene oxide reduction [80]. The successful development of future graphene-based electronic devices depends on high-quality and the large scale availability of the material [4,70,81–83].

As predicted by Geim and Novoselov [70], the most immediate application for graphene could be integration in composite materials. However, preparation of graphene-based composite materials is not a trivial task due to the strong surface-surface attraction between the sheets preventing its dispersion. Moreover, depending on the method of preparation the transport properties of few graphene layers can be considerably reduced as compared to expected properties of single layer material. To illustrate this, Fig. 4 shows an example of resistivity measurements performed on a flake agglomerate graphene sheets sample chemically derived from graphite oxide. Between 6 K and 200 K, the resistivity as a function of temperature clearly exhibits a VHR law $\rho = \rho_0 \exp\left(\frac{T_0}{T}\right)^x$ with $x = 0.52$ characteristic of 1D conductivity according to Mott model. Such a behavior is difficult to explain for flake agglomerate 2D graphene sheets. As discussed above, the 1D VHR conductivity is often observed in amorphous carbon materials [10]. The effects of electron-electron interaction on disordered systems with highly localized states leading to a $T^{-1/2}$ dependence have been early investigated by Efros and Shklovskii [84]. Evidence of Coulomb gap in agglomerate graphene sheets derived from graphite oxide needs more investigation.

Graphene can be used in nanocomposite conducting polymers, Stankovich et al. [85] have succeeded to prepare polystyrene-graphene composites with excellent structural characteristics where the graphene sheets were individually and uniformly distributed throughout the volume, such composites exhibit very low percolation

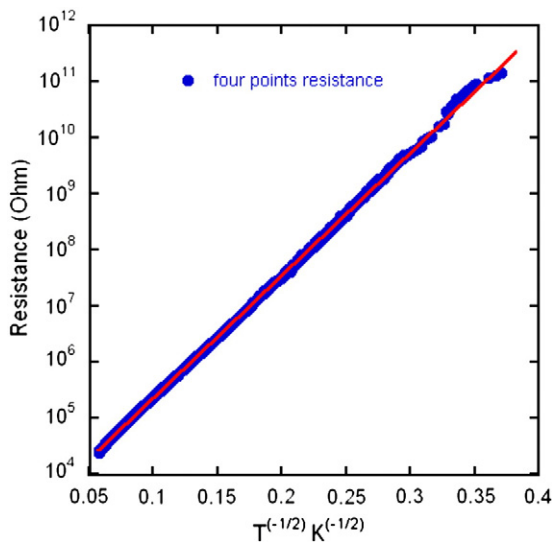


Fig. 4. Sheet resistance of graphene packet layers produced by chemical reducing graphite oxide. $\ln(R)$ is presented as function of $T^{-1/2}$, in order to evidence the modified VHR behaviour. The line is a guide for the eyes. The best fits give $x = 0.521$.

threshold of around 0.1 vol.% and high electrical conductivity of about 0.1 Sm^{-1} enough for many electrical applications. Graphene thin films can also be used as transparent electrodes for solar cells [86] or in liquid crystal devices [87]. Another interesting field of application for graphene-based composites is in Li-ion batteries. Recently Paek et al. have [88] reported on the preparation tin oxide/graphene nanosheets (SnO_2/GNS) nanocomposites, the SnO_2/GNS nanoporous material exhibits reversible capacity of 810 mAh/g with superior cyclic performances compared to that of bare SnO_2 nanoparticles.

6. Carbon blacks

Carbon black (CB) is the generic name for a family of small particle size carbon fractal aggregates. Carbon black is chemically and physically distinct from soot and black carbon. The basic building units of CB are nano-sized particles formed by stacked graphene layers exhibiting random orientations about the stacking axis and also in translation parallel to the layers (turbostratic structure). The graphene layers contain defects, distortions and discontinuities. Some graphene layers extend over two adjacent particles. The overlapping graphene layers and the fused nature of the particles ensure the electrical conductivity throughout the aggregate structure [89–91]. Carbon blacks are electrical conductors with electrical conductivity values ranging from 1 to 10^4 S/m . The intrinsic electrical properties of CB aggregates depend on many factors such as the electrical conductivity and the size of the individual particles, the level and nature of impurities on the surface of the graphene layers, the degree of contact between the particles of the same aggregate and between the particles of different aggregates, and the packing factor or density [92–96].

Due to their electrical properties, carbon blacks are widely used as conducting fillers in polymers. CB/polymer composites have wide range of applications including graded semiconductors for optoelectronic applications, conducting electrodes, solid electrolytes for batteries, anti-reflection coatings, room temperature gas sensors, electrical switching devices, etc. The electrical applications of CB have been reviewed recently by Chung [97]. It is worth noting that most of CB/polymer composites exhibit a sharp increase of their electrical resistivity with increasing the temperature. This phenomenon, known as the positive temperature coefficient PTC effect, is particularly pronounced in semicrystalline polymers near the melting point [98–100]. In addition, drastic increase of the resistivity (10^3 – 10^6 times) can also be observed at room temperature when CB/polymer composites are exposed to solvent vapours (acetone, butanone, chloroform, cyclohexane, benzene, toluene) [101,102]. Both the PTC and the chemiresistive effects have been described on the basis of percolation theory; the matrix expansion and the breakdown of conduction pathways throughout the composite play the main role.

7. Conclusions

There is no doubt that carbon based nanocomposite materials will be used in the future in numerous applications. The combination of pure organic, inorganic, biological materials with carbon should result in new materials with superior physical and chemical properties. From the electronic point of view, carbon based nanocomposites can be insulators, semiconductors, metals and superconductors offering to engineers the opportunity to use them in a wide range of applications. The electrical properties of carbon based composite materials are intimately related to the electronic properties and the nature of their constituting components. Obviously, one of the greatest challenges for future industrial applications is better carbon materials synthesis with improved reproducibility. In particular, the control of the size, defect density and doping of the nanostructures is a necessity.

Regarding the preparation methods, surprisingly physical or chemical vapor deposition (PVD, CVD) techniques have very little

explored as alternative methods for the preparations of conductive C based nanocomposite thin films which constitute interesting materials for many industrial applications. PVD and CVD techniques combine with standard chemical and other methods can be used for the deposition of the filler or matrix phase in single layer nanocomposite thin films or for the deposition of advanced nanocomposite multilayer thin films with special nano-architecture such as multilayers composed of thin layers of different C based nanocomposite materials.

Acknowledgments

The authors gratefully acknowledge the financial support of the Swiss Science Foundation and of the Ecole Polytechnique Fédérale de Lausanne. Part of the work was funded by the European projects VIACARBON and MULTIPLAT as well as by the Nano Tera project CABTURE.

References

- [1] G.L. Hornyak, H.F. Tibbals, J. Dutta, J.J. Moore, Introduction to Nanoscience and Technology, CRC Press, NY, 2009.
- [2] H. Kuzmany, J. Fink, M. Mehring, S. Roth (Eds.), Electronic Properties of Novel Materials – Molecular Nanostructures, AIP Conference Proceedings, vol. 544, 2000.
- [3] M.S. Dresselhaus, G. Dresselhaus, P. Avouris, Carbon Nanotubes: Synthesis, Structure, Properties and Applications, vol. 80, Springer, Berlin, 2001.
- [4] P. Avouris, Z. Chen, V. Perebeinos, Nat. Nanotechnol. 2 (2007) 605.
- [5] J.J. Hauser, J. Non-Cryst. Solids 23 (1977) 21.
- [6] M. Morgan, Thin Solid Films 7 (1971) 313.
- [7] B. Meyerson, F.W. Smith, J. Non-Cryst. Solids 35 (36) (1980) 435.
- [8] E. Staryga, G.W. Bak, Diamond Relat. Mater. 14 (2005) 23.
- [9] N.F. Mott, E.A. Davis, Electronic Processes in Non-Crystalline Materials, Clarendon Press, Oxford, 1979.
- [10] J.G. Zhao, L.X. Yang, F.Y. Li, R.C. Yu, C.Q. Jin, Solid State Sci. 10 (2008) 1947.
- [11] F. Alibart, O. Durand Drouhin, M. Lejeune, M. Benlahsen, S.E. Rodil, E. Camps, Diamond Relat. Mater. 17 (2008) 925.
- [12] K. Shimikawa, K. Miyake, Phys. Rev. B 39 (1989) 7578.
- [13] C. Godet, J.P. Kleider, A.S. Gudovskikh, Diamond Relat. Mater. 16 (2007) 1799.
- [14] N. Konofao, C.T. Angelis, E.K. Evangelou, C.A. Dimitriadis, S. Logothetidis, Appl. Phys. Lett. 79 (2001) 2381.
- [15] P.N. Vishwakarma, S.V. Subramanyam, J. Appl. Phys. 100 (2006) 113702.
- [16] C. Ducati, E. Barborini, P. Piseri, P. Milani, J. Robertson, J. Appl. Phys. 92 (2002) 5482.
- [17] D.H. Zhong, H. Sano, Y. Uchiyama, K. Kobayashi, Carbon 38 (2000) 1199.
- [18] A. Sikora, A. Berkesse, O. Bourgeois, J.-L. Garden, C. Guerret-Piécourt, J.-N. Rouzaud, A.-S. Loir, F. Garrelie, C. Donnet, Solid State Sci. 11 (2009) 1738.
- [19] B. Xue, P. Chen, Q. Hong, J. Lin, K.L. Tan, J. Mater. Chem. 11 (2001) 2378.
- [20] V. Georgakilas, D. Gournis, V. Tzitzios, L. Pasquato, D.M. Guldi, M. Prato, J. Mater. Chem. 17 (2007) 2679.
- [21] S. Papadimitriou, A. Tegou, E. Pavlidou, S. Armanyanov, E. Valova, G. Kokkinidis, S. Sotiropoulos, Electrochim. Acta 53 (2008) 6559.
- [22] A. Kuwahara, S. Suzuki, M. Miyayama, Solid State Ionics 179 (2008) 1890.
- [23] A. Nigro, G. Nobile, M.G. Rubino, R. Vaglio, Phys. Rev. B 37 (1988) 3970.
- [24] M.D. Abad, J.C. Sánchez-López, N. Cusnir, R. Sanjinés, J. Appl. Phys. 105 (2009) 033510.
- [25] C. Hierold, A. Jungen, C. Stamfer, T. Helbling, Sens. Actuators A 136 (2007) 51.
- [26] P. Sharma, P. Ahuja, Mater. Res. Bull. 43 (2008) 2517.
- [27] S. Daniel, T.P. Rao, K.S. Rao, S.U. Rani, G.R.K. Naidu, H.-Y. Lee, T. Kawai, Sens. Actuators B 122 (2007) 672.
- [28] C. Li, E.T. Thostenson, T.-W. Chou, Compos. Sci. Technol. 68 (2008) 1227.
- [29] M. Mionić, D.T.L. Alexander, L. Forró, A. Magrez, Phys. Status Solidi B 245 (2008) 1915.
- [30] R. Smajda, M. Mionic, M. Duchamp, J.C. Andresen, L. Forró, A. Magrez, Phys. Status Solidi C 7 (2010) 1236.
- [31] R. Smajda, J.C. Andresen, M. Duchamp, R. Meunier, S. Casimirius, K. Hernadi, L. Forró, A. Magrez, Phys. Status Solidi B 7 (2009) 2457.
- [32] I. Balberg, D. Azulay, D. Tokor, O. Millo, Int. J. Mod. Phys. B 18 (15) (2004) 2091.
- [33] N. Grossiord, P.J.J. Kivit, J. Loos, J. Meuldijk, A.V. Kyrilyuk, P. van de Schoot, C.E. Koning, Polymer 49 (2008) 2866.
- [34] W. Bauhofer, J.Z. Kovacs, Compos. Sci. Technol. 69 (2009) 1486.
- [35] K. Widney, T. Kasiwagi, M. Mu, MRS Bull. 32 (2007) 348.
- [36] B. Krause, P. Pötschke, L. Häußler, Compos. Sci. Technol. 69 (2009) 1505.
- [37] J. Li, P.C. Ma, W.C. Chow, C.K. To, B.Z. Tang, J.K. Kim, Adv. Funct. Mater. 17 (2007) 3207.
- [38] J.K.W. Sandler, J.E. Kirk, I.A. Kinloch, M.S.P. Shaffer, A.H. Windle, Polymer 44 (2003) 5893.
- [39] A. Moissala, Q. Li, I.A. Kinloch, A.H. Windle, Compos. Sci. Technol. 66 (2006) 1285.
- [40] A. Buldum, J.P. Lu, Phys. Rev. B 63 (2001) 161403-1-4.
- [41] M. Stadermann, S.J. Papadakis, M.R. Falvo, J. Novak, E. Snow, Q. Fu, J. Liu, Y. Fridman, J.J. Boland, R. Superfine, S. Washburn, Phys. Rev. B 69 (2004) 201402-1-3.
- [42] P.C. Ma, B.Z. Tang, J.-K. Kim, Carbon 46 (2008) 1497.
- [43] F. Du, J.E. Fischer, K.I. Winey, Phys. Rev. B 72 (2005) 121204-1.
- [44] G.G. Silva, M.F. Rodrigues, C. Fantini, R.S. Borges, M.A. Pimenta, B.J. Carey, L. Cie, P.M. Ajayan, Macromol. Mater. Eng. 295 (2010), doi:10.1002/mame.201000276.
- [45] H. Ago, K. Petritsch, M.S.P. Shaffer, A.H. Windle, R.H. Friend, Adv. Mater. 11 (1999) 1281.
- [46] S.R. Forrester, Nature 428 (2004) 911.
- [47] J.V.D. Lagemaat, T.M. Barnes, G. Rumbles, S.E. Shaheen, T.J. Coutts, C. Weeks, I. Levitsky, J. Peltola, P. Glatkowski, Appl. Phys. Lett. 88 (2006) 233503.
- [48] C.M. Aguirre, S. Auvray, S. Pigeon, R. Izquierdo, R. Martel, Appl. Phys. Lett. 88 (2006) 183104.
- [49] M.W. Rowell, M.A. Topinka, M.D. McGehee, H.-J. Prall, G. Dennler, N.S. Sariciftci, L. Hu, G. Gruner, Appl. Phys. Lett. 88 (2006) 233506.
- [50] E. Kymakis, I. Alexandrou, G.A.J. Amaratunga, J. Appl. Phys. 93 (2003) 1764.
- [51] S.P. Somani, P.R. Somani, M. Umeno, Diamond Relat. Mater. 17 (2008) 585.
- [52] D.J. Guo, H.L. Li, Carbon 43 (2005) 1259.
- [53] H.P. Wu, X.J. Wu, M.Y. Ge, G.Q. Zhang, Y.W. Wang, J. Jiang, Compos. Sci. Technol. 67 (2007) 1182.
- [54] S.B. Yan, H.H. Song, X.H. Chen, A.V. Okotrub, L.G. Bulusheva, Electrochim. Acta 52 (2007) 5286.
- [55] J. Shu, H. Li, R.Z. Yang, Y. Shi, X.J. Huang, Electrochim. Commun. 8 (2006) 51.
- [56] W.X. Chen, J.Y. Lee, Z.L. Liu, Carbon 41 (2003) 959.
- [57] J. Yan, H. Song, S. Yang, J. Yan, X. Chen, Electrochim. Acta 53 (2008) 6351.
- [58] P.G. Collins, K. Bradley, M. Ishigami, A. Zettl, Science 287 (2001) 1801.
- [59] J. Kong, N.R. Franklin, C. Zhou, M.G. Chapline, S. Peng, K. Shio, H. Dai, Science 287 (2000) 622.
- [60] A. Modi, N. Koratkar, E. Lass, B.Q. Wei, P.M. Ajayan, Nature 424 (2003) 171.
- [61] T. Someya, J. Small, P. Kim, C. Nuckolls, J.T. Yardley, Nano Lett. 3 (2003) 877.
- [62] O.K. Varghese, P.D. Kichambre, D. Gong, K.G. Ong, E.C. Dickey, C.A. Grimes, Sens. Actuators B Chem. 81 (2001) 32.
- [63] J. Chung, K.H. Lee, J.H. Lee, D. Troya, G.C. Schatz, Nanotechnology 15 (2004) 1596.
- [64] E.S. Snow, F.K. Perkins, E.J. Houser, S.C. Badescu, T.L. Reinecke, Science 307 (2005) 1942.
- [65] A. Star, V. Joshi, S. Skarupo, D. Thomas, J.-C.P. Gabriel, J. Phys. Chem. B 110 (2006) 21014.
- [66] Y. Lu, J. Li, J. Han, H.T. Ng, C. Binder, C. Partridge, M. Meyyapan, Chem. Phys. Lett. 391 (2004) 344.
- [67] C.H. Wang, Y. Li, M.J. Yang, Sens. Actuators B 124 (2007) 360.
- [68] L. Valentini, V. Bavastrello, E. Stura, I. Armentano, C. Nicolini, J.M. Kenny, Chem. Phys. Lett. 383 (2004) 617.
- [69] K.H. An, S.Y. Jeong, H.R. Hwang, Y.H. Lee, Adv. Mater. 16 (2004) 1005.
- [70] A.K. Geim, K.S. Novoselov, Nat. Mater. 6 (2007) 183.
- [71] K.S. Novoselov, A.K. Geim, S.V. Morozov, D. Jiang, Y. Zhang, S.V. Dubonos, I.V. Grigorieva, A.A. Firsov, Science 306 (2004) 666.
- [72] K.I. Bolotin, K.J. Sikes, Z. Jiang, G. Funderberg, J. Hones, P. Kim, H.L. Stormer, Solid State Commun. 146 (2008) 351.
- [73] C. Berger, Z.M. Song, B.X. Li, X.S. Wu, N. Brown, C. Naud, D. Mayo, T.B. Li, J. Hass, A.N. Marchenkov, E.H. Conrad, P.N. First, W.A. de Heer, Science 312 (2006) 1191.
- [74] T. Yokoyama, Phys. Rev. B 77 (2008) 073413.
- [75] F. Schedin, A.K. Geim, S.V. Morozov, E.W. Hil, P. Blake, M.I. Katsnelson, K.S. Novoselov, Nat. Mater. 6 (2007) 652.
- [76] V.I. Fal'ko, Nat. Phys. 3 (2007) 151.
- [77] H. Ueta, M. Saida, C. Nakai, Y. Yamada, M. Sasaki, S. Yamamoto, Surf. Sci. 560 (2004) 183.
- [78] N. Gall, E. Rut'kov, A. Tontegode, Phys. Solid State 46 (2004) 371.
- [79] S. Marchini, S. Gunther, J. Wintterlin, Phys. Rev. B Condens. Matter 76 (2007) 075429.
- [80] G. Eda, G. Fanchini, M. Chhowalla, Nat. Nanotechnol. 3 (2008) 270.
- [81] X. Li, W. Cai, J. An, S. Kim, J. Nah, D. Yang, R. Piner, A. Velamakanni, I. Jung, E. Tutuc, S.K. Banerjee, L. Colombo, R.S. Ruoff, Science 324 (2009) 1312.
- [82] K.S. Kim, Y. Zhao, H. Jang, S.Y. Lee, J.M. Kim, K.S. Kim, J.-H. Ahn, Ph. Kim, J.-Y. Choi, B.H. Hong, Nature 457 (2009) 706.
- [83] K.V. Emtsev, A. Bostwick, K. Horn, J. Jobst, G.L. Kellogg, L. Ley, J.L. McChesney, T. Ohta, S.A. Reshanov, J. Röhrl, E. Rotenberg, A.K. Schmid, D. Waldmann, H.B. Weber, T. Seyller, Nat. Mater. 8 (2009) 203.
- [84] A.L. Efros, B.S. Shklovskii, J. Phys. C Solid State Phys. 8 (1975) L49.
- [85] S. Stankovich, D.A. Dikin, G.H.B. Dommett, K.M. Kohlhaas, E.J. Zimney, E.A. Stach, R.D. Piner, S.T. Nguyen, R.S. Ruoff, Nature 442 (2006) 282.
- [86] X. Wang, L. Zhi, K. Müllen, Nano Lett. 8 (2008) 323.
- [87] P. Blake, P.D. Brimicombe, R.R. Nair, T.J. Booth, D. Jiang, F. Schedin, L.A. Ponomarenko, S.V. Morozov, H.F. Gleeson, E.W. Hil, A.K. Geim, K.S. Novoselov, Nano Lett. 8 (2008) 1704.
- [88] S.-M. Paek, E. Yoo, I. Honma, Nano Lett. 9 (2009) 72.
- [89] X. Bourrat, Carbon 31 (1993) 287.
- [90] W.M. Hess, C.R. Herd, in: J. Donnet, R.C. Bansal, M. Wang (Eds.), Carbon Black Science and Technology, 2nd ed., Marcel Dekker, NY, USA, 1993, p. 89.
- [91] J.R. Nelson, W.K. Wissing, Carbon 24 (1986) 115.
- [92] N. Probst, in: J. Donnet, R.C. Bansal, M. Wang (Eds.), Carbon Black Science and Technology, 2nd ed., Marcel Dekker, NY, USA, 1993, p. 271.
- [93] D. Pantea, H. Darmstadt, S. Kaliaguine, L. Sümmchen, C. Roy, Carbon 39 (2001) 1147.
- [94] L. Salome, F. Carmona, Carbon 29 (1991) 599.

- [95] F. Ehrburger-Dolle, J. Lahaye, S. Misono, Carbon 32 (1994) 1363.
- [96] J. Sánchez-González, A. Marcías-García, M.F. Alexandra-Franco, V. Gómez-Serrano, Carbon 43 (2005) 741.
- [97] D.D.L. Chung, J. Mater. Sci. 39 (2004) 2645.
- [98] M. Hindermann-Bischoff, F. Ehrburger-Dolle, Carbon 39 (2001) 375.
- [99] A. Voet, Rubber Chem. Technol. 54 (1981) 42.
- [100] C. Zhang, C.A. Ma, P. Wang, M. Sumita, Carbon 43 (2005) 2544.
- [101] B.J. Doleman, M.C. Lonergan, E.J. Severin, T.P. Vaid, N.S. Lewis, Anal. Chem. 70 (1998) 4177.
- [102] J. Chen, N. Tsubokawa, Y. Maekawa, M. Yoshida, Carbon 40 (2002) 1602.